

# Collisional removal of OH ( $X^2\Pi, \nu=7$ ) by $O_2$ , $N_2$ , $CO_2$ , and $N_2O$

Karen Knutsen,<sup>a)</sup> Mark J. Dyer,<sup>b)</sup> and Richard A. Copeland  
SRI International, Molecular Physics Laboratory, Menlo Park, California 94025

(Received 15 November 1995; accepted 11 January 1996)

Collisional removal rate constants for the OH ( $X^2\Pi, \nu=7$ ) radical are measured for the colliders  $O_2$ ,  $CO_2$ , and  $N_2O$ , and an upper limit is established for  $N_2$ . OH( $\nu=4$ ) molecules, generated in a microwave discharge flow cell by the reaction of hydrogen atoms with ozone, are excited to  $\nu=7$  by the output of a pulsed infrared laser via direct vibrational overtone excitation. The temporal evolution of the  $\nu=7$  population is probed as a function of the collider gas partial pressure by a time-delayed pulsed ultraviolet laser. The probe laser light is resonant with the (0,7) band of the  $B^2\Sigma^+ - X^2\Pi$  transition. Fluorescence from the  $B^2\Sigma^+$  state is detected in the visible spectral region. We measure rate constants for  $CO_2$ ,  $(6.7 \pm 1.0) \times 10^{-11}$ ;  $N_2O$ ,  $(3.0 \pm 0.6) \times 10^{-11}$ ;  $O_2$ ,  $(7 \pm 2) \times 10^{-12}$ ; and  $N_2$ ,  $< 6 \times 10^{-13}$  (all in units of  $cm^3 s^{-1}$ ). © 1996 American Institute of Physics. [S0021-9606(96)01115-9]

## INTRODUCTION

Vibrationally excited OH radicals are generated in the upper mesosphere near 90 km by the reaction of hydrogen atoms with ozone.<sup>1</sup> Once produced, the hydroxyl radical can either fluoresce or be deactivated in collisions with the ambient species:  $O_2$ ,  $N_2$ , and O atoms. Over the past decade, significant progress has been made in measuring the vibrational level dependence of the total removal rate constants for these collisional processes in the laboratory.<sup>2-10</sup> Upon examination of the existing experimental data on this relaxation, we found no reliable measurements of the total removal rate constants for the vibrational levels  $\nu=7$  and 8. Because of the pressure conditions in the atmosphere, these levels are extremely important in the modeling of the Earth's nightglow.<sup>11,12</sup> Moreover, these levels connect the measurements for low vibrational levels ( $\nu \leq 6$ ) made by Dodd *et al.*<sup>7,8</sup> and the measurements made for  $\nu=9$  and 12 made in this laboratory,<sup>6,10,13,14</sup> providing a consistency check for the recent laboratory data. In this work we apply the technique used in the study of  $\nu=9$  by Chalamala and Copeland<sup>10</sup> to the  $\nu=7$  vibrational level.

Complete review of the extensive literature of the relaxation of OH vibrational levels can be found in several manuscripts and will only be summarized here.<sup>2,8,14</sup> Early experiments were unreliable because of difficulties with the experimental approach.<sup>2,3</sup> Simply put, the reactions that generated the vibrationally excited OH were slower than the reactions that removed it. This made the kinetic modeling of reactive-production-based systems very complicated. The experimental problems were described by Finlayson-Pitts and Kleindienst<sup>2</sup> (FPK) and Greenblatt and Wiesenfeld.<sup>3</sup> Disregarding the work done before 1981, more recent direct measurements have been very consistent. FPK began the contemporary measurements by using a discharge flow tube to

measure the relative rate constants for the colliders  $O_2$ ,  $CO_2$ , Ar, and  $N_2$  for  $\nu=9$ . For the atmospheric gases, they found that  $O_2$  is at least 20 times more efficient at relaxing  $\nu=9$  than  $N_2$ . Absolute rate constants could only be obtained by assuming a value for the  $A_{9,3}$  Einstein coefficient which, to this date, is still highly variable in the literature.<sup>12</sup> Direct measurements for vibrational levels greater than one began with the study of vibrational relaxation in  $\nu=2$  via vibrational overtone excitation from the ground vibrational state.<sup>4,5</sup> Measurements have been made for  $\nu=2$  for  $O_2$  and upper limits extracted for  $N_2$  along with data for many other colliders. Dodd *et al.*<sup>7,8</sup> in two publications made measurements for a range of vibrational levels spanning one to six for  $O_2$  as a collider and one to four for  $CO_2$ . They used 35 kV electron beam excitation and modeled the relaxation of the product vibrational distribution assuming different relaxation mechanisms. For  $\nu=2$ , the extracted results for  $O_2$  collisions are consistent with the results from direct overtone excitation.<sup>4,5</sup> They concluded that a single quantum vibrational cascade mechanism was consistent with their data for these vibrational levels. At the same time as the Dodd *et al.* study, Copeland and co-workers began experiments on high vibrational levels of OH. Initial experiments<sup>6</sup> were performed on the  $\nu=12$  level, which is higher in energy than those levels populated in the earth's atmosphere by the hydrogen atom reaction with ozone. These measurements yielded rate constants significantly faster than any recorded previously for OH ground state vibrational removal and showed that the difference between the  $O_2$  and the  $N_2$  rate constants decreased with increasing vibrational level. The most recent experiments involved  $\nu=9$ , the highest lying vibrational level populated by the OH( $\nu$ ) production reaction.<sup>10</sup> OH vibrational removal measurements again showed very rapid removal, with ratios of the collider rate constants consistent with the FPK study.<sup>2</sup> Given all these measurements, we were left with one atmospherically important experimental gap in the measurements between the  $\nu=6$  measurements of Dodd *et al.*<sup>8</sup> and the  $\nu=9$  measurements of this laboratory.<sup>10</sup>

Understanding the relaxation process in these high vibra-

<sup>a)</sup>Present address: Battelle Pacific NW Laboratories, P.O. Box 999, MS K2-14, Richland, Washington 99352.

<sup>b)</sup>Present address: JILA, Room S370, Campus Box 440, Boulder, Colorado 80309-0440.

tional levels ( $9 > \nu > 6$ ) is particularly important in modeling the vibrational and altitude dependence of the earth's nightglow. In 1987, McDade and Llewellyn proposed several limiting mechanisms through which the OH vibrational relaxation might proceed.<sup>11</sup> These mechanisms were the single quantum cascade model, where the OH molecules are collisionally deactivated in one-quantum steps in the OH vibrational quantum number, and the sudden death model, where all the excited OH undergo either complete deactivation or reaction in one removal collision. By comparing the distribution of vibrational levels observed in the atmosphere with kinetic model results, they concluded that if single quantum cascade was valid for all vibrational levels, there had to be a maximum in the removal rate constant at  $\nu=7$ . For the "sudden death" model, such a maximum in the removal rate constant was not needed. Clearly,  $\nu=7$  experimental values are needed to either support or contradict the proposed relaxation pathways.

In this work, we use a similar approach to the two previous SRI studies. Vibrationally excited OH ( $5 \leq \nu \leq 9$ ) are produced via a reaction of hydrogen atoms and ozone in a discharge flow cell. Using a pulsed infrared laser, some of the ground electronic state  $\nu=4$  radicals are excited to a specific rotational state in  $\nu=7$  via a direct overtone vibration excitation. The time dependence of the  $\nu=7$  population is examined by a time-delayed pulsed ultraviolet laser. The probe laser light excites the OH( $\nu=7$ ) to the  $B^2\Sigma^+$  electronic state, and a filtered photomultiplier tube monitors the fluorescence to the  $A^2\Sigma^+$  state.<sup>15,16</sup> The rate constants obtained from the temporal evolution are compared to earlier studies, and a consistent picture is obtained for the collisional energy transfer from  $\nu=1$  to 12.

## EXPERIMENTAL APPROACH

The details of the experimental approach begin with a description of the OH production. The reaction of  $O_3$  with H atoms produces vibrationally excited OH in the flow cell. A microwave discharge generates H atoms from a gas mixture consisting of 20–30 standard cubic centimeter per minute (sccm) flow of  $H_2$  seeded in 1000 sccm flow of He. Downstream of the microwave discharge cavity, the glass discharge tube consists of a 3.8 cm diameter outer tube, through which the H/He mixture flows, and a concentric 0.635 cm diameter tube inlet, through which the  $O_3$  is introduced. The reactants mix only after entering the cell, over a distance of 4 cm to the OH observation region. The  $O_3$  is produced by a commercial ozonator and trapped in silica gel (grade 40) at 196 K. A He pressure slightly higher than atmospheric pressure produces a flow of 300–600 sccm of He through the ozone trap. This He flow entrains the  $O_3$  and carries it into the flow cell. The various colliders are introduced by mixing them with either the  $O_3$ /He or H/He gas flows in the discharge tube, from 15–20 cm upstream of the cell. All gas flows are measured with calibrated mass flow meters. The total pressure is measured with a capacitance manometer. From the flow rates and total pressure, the partial pressure of

each is obtained; total cell pressure of up to 7 Torr, and collider partial pressures of up to 2.5 Torr, are used.

OH radicals in  $\nu=5-9$  are produced by the  $O_3+H$  reaction. In order to prepare  $\nu=7$  by the  $(X^2\Pi-X^2\Pi)$  (7,4) overtone excitation, this distribution of vibrational states must first be collisionally relaxed to lower levels. Ideally, one would like to start with all of the population in  $\nu=4$ , and none in  $\nu=7$ , so that only the laser-prepared  $\nu=7$  population is detected by the  $B^2\Sigma^+-X^2\Pi$  laser-induced fluorescence (LIF). To optimize the  $\nu=4/\nu=7$  ratio, we vary the total cell pressure and the position of the gas inlet ports with respect to the observation region, and add different gases to enhance the relaxation process while observing the OH( $\nu=7$ ) laser-induced fluorescence signal both on and off of the (7,4) resonance. At short time delays, before the prepared rovibrational state has had time to rotationally equilibrate, the on-resonance: off-resonance signal ratio taken probing the prepared level is a maximum of 3.5:1. Rotational equilibration of the prepared vibrational state occurs on a time scale that is fast compared to the collisional removal of the vibrational state. Data are obtained by probing a rotational level that is filled by the rotational equilibration process, to minimize the effect of this rotational equilibration on the measurement of the vibrational removal rate constant. To this end, we prepare OH( $\nu=7$ ) through excitation of  $(X^2\Pi-X^2\Pi)$  (7,4)  $Q_1(1)$  transition, and monitor the population by LIF through excitation of  $(B^2\Sigma^+-X^2\Pi)$  (0,7)  $Q_1(3)$ .<sup>17</sup> Due to rotational equilibration, the on-resonance: off-resonance signal ratio drops below 1.5:1. Since noise on the off-resonance signal is about 10%, this signal is still 2–5 times the background noise level.

The excitation and detection lasers are counter propagated and overlapped in the flow cell. Since the two-laser signal is a sensitive function of this overlap, the beam sizes are matched. Both beams are focused into the center of the cell by 1 m lenses. To excite the  $(X^2\Pi-X^2\Pi)$  (7,4) overtone, the output of a 10 Hz Nd:YAG-pumped dye laser is Raman shifted in 350 psi of  $H_2$ . The second Stokes output near 1200 nm, typically 5 mJ/pulse, is separated from the fundamental by a stack of two long-pass glass filters. Reflective loss is minimized by using infrared mirrors to direct the Raman-shifted light into the center of the flow cell. The wavelength of the laser light is tuned to excite the  $Q_1(1)$  transition of the  $(X^2\Pi-X^2\Pi)$  (7,4) band. The frequency-doubled output of an excimer-pumped dye laser, also run at 10 Hz, is tuned to detect the prepared OH( $\nu=7$ ) using the  $B^2\Sigma^+-X^2\Pi$  (0,7) band near 213 nm (at typically 0.4 mJ/pulse). The resulting  $(B^2\Sigma^+-A^2\Sigma^+)$  fluorescence is collected at right angles with a photomultiplier tube (Hamamatsu R105), where two glass filters (Schott GG-420) and a long-pass filter (Corion LS-600-F-K220) isolate the  $(B^2\Sigma^+-A^2\Sigma^+)$  (0,6), (0,7), and (0,8) bands in emission (450–570 nm) and eliminate scattered light from both lasers. The analog output of the photomultiplier is fed into a gated integrator and stored on computer.

To obtain the temporal evolution of the OH( $\nu=7$ ) population, the time delay between the excitation and detection lasers is scanned. Data are collected over time delays up to

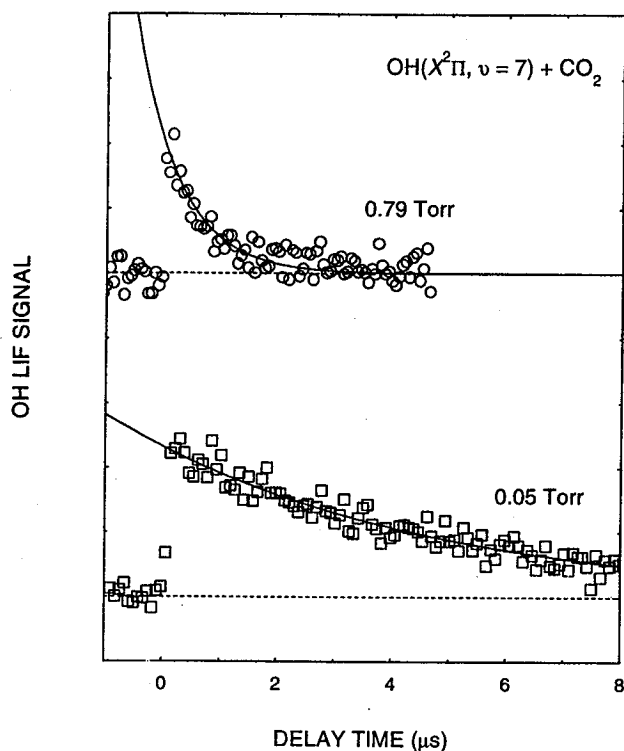


FIG. 1. Time dependence of the OH ( $\nu=7$ ) population as a function of  $\text{CO}_2$  partial pressure. The squares are the experimental data points at 0.05 Torr of added  $\text{CO}_2$  and the circles are the points at 0.79 Torr of added  $\text{CO}_2$ . The solid lines are the best fit single exponential and the dashed line the best fit baseline.

20  $\mu\text{s}$ , depending upon the collider pressure and removal efficiency, averaging 140 laser shots per time delay setting. The colliders and their partial pressures are then varied to produce the desired rate constant information.

## RESULTS

Figure 1 shows typical experimental data for  $\nu=7$  at 0.05 and 0.79 Torr of added  $\text{CO}_2$ . The solid line is the best fit single exponential and the dashed line is the fit to the background  $\nu=7$  signal. In most cases the signal is fit from approximately 80% of the peak intensity until the end of the data. Decay constants for these experimental data are plotted vs the partial pressure of added collider. The results for  $\text{CO}_2$ ,  $\text{N}_2\text{O}$ ,  $\text{O}_2$ , and  $\text{N}_2$  are shown in Fig. 2. From Fig. 2 we see that  $\text{CO}_2$  is the most efficient at removing the  $\nu=7$  OH, and  $\text{N}_2$  is the least efficient. The data for  $\text{N}_2$  extends to much higher pressure but is not included in the figure so that the scatter in the other colliders can be illustrated. All reported rate constants are from weighted linear-least-squares fits to the experimental data, and the quoted error values are two standard deviations to the linear fit. Unweighted fits differ slightly in the absolute magnitude of the rate constant but always overlap within the error estimates. The data for  $\text{CO}_2$  shows significantly more scatter since it is used as a test gas for the degree of mixing as described later.

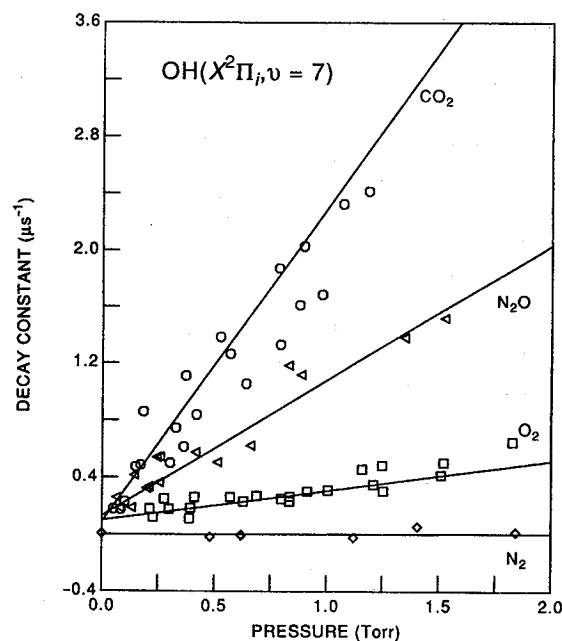


FIG. 2. Pressure dependence of the OH ( $\nu=7$ ) signal decay constant for  $\text{CO}_2$ ,  $\text{N}_2\text{O}$ ,  $\text{O}_2$ , and  $\text{N}_2$ . The circles are  $\text{CO}_2$ , the triangles  $\text{N}_2\text{O}$ , the squares  $\text{O}_2$ , and the diamonds  $\text{N}_2$ . The solid lines are the results of a weighted linear least squares fit to the data points. Additional points at higher pressure of  $\text{N}_2$  are not displayed.

As with any reactive flow tube study, complete mixing is critical to accurate measurements. For our experiments, we are slightly less demanding on how quickly the mixing occurs. In these experiments, the species must be well mixed by the region of laser excitation and detection because to obtain the partial pressure of the collider in the observation region all the individual flows are added together and the partial pressure calculated from the individual flows and the total pressure. All mixing checks are performed with  $\text{CO}_2$ , since it gave the largest signals and permitted more variation in the flow conditions while maintaining a sufficient signal for analysis.

We checked for systematic errors in the rate constant measurements due to mixing effects by comparing rate coefficients obtained with  $\text{CO}_2$  collider entering through the  $\text{O}_3$  inlet, the H inlet, and with the partial flows of  $\text{CO}_2$  balanced through both inlets. The slopes obtained from plotting these data varied in an apparently random manner with their respective uncertainties, so we conclude there is no systematic error due to choice of collider inlet, and therefore mixing. The average of the different slopes is the same as the slope obtained by fitting all of the data points as a group, and the latter value is the one we report for the  $\text{CO}_2$  rate constant.

For the  $\text{O}_2$  collider, the measurements are taken by addition through the  $\text{O}_3$  inlet. This gave the maximum partial pressure range while maintaining the signal intensity. For  $\text{N}_2$ , a small amount of  $\text{N}_2\text{O}$  is added to enhance the population difference between  $\nu=4$  and 7. The slope of the line for the decay constant versus added  $\text{N}_2$  partial pressure is not significantly different from zero, therefore we report a two stan-

TABLE I. OH ( $X^2\Pi_i, \nu=7$ ) vibrational relaxation rate constants. All error estimates are two standard deviations and the upper limit for  $N_2$  is a two standard deviation upper limit.

Collider	$k$ ( $\text{cm}^3 \text{s}^{-1}$ )	$\sigma$ ( $\text{\AA}^2$ )
$\text{CO}_2$	$6.7 \pm 1.0 \times 10^{-11}$	$11 \pm 2$
$\text{N}_2\text{O}$	$3.0 \pm 0.6 \times 10^{-11}$	$5.2 \pm 1.0$
$\text{O}_2$	$7 \pm 2 \times 10^{-12}$	$1.1 \pm 0.3$
$\text{N}_2$	$< 6 \times 10^{-13}$	$< 0.09$

dard deviation upper limit. Table I contains the rate constants measured in this study and the thermally averaged collision cross sections calculated using the root mean-squared velocity.

## DISCUSSION

These rate constants are part of a large body of information on OH vibrational relaxation, and their significance lies in the coupling with previous measurements and atmospheric modeling. Given the relative magnitude of the  $\text{O}_2$  and  $\text{N}_2$  rate constants, it is clear that OH removal in the atmosphere for the high vibrational levels is dominated by collisions with  $\text{O}_2$ . Lower levels may be influenced by O-atom collisional relaxation. The O-atom concentration is about a factor of 100 lower than the  $\text{O}_2$  concentration at the altitude of the OH emission in the earth's atmosphere. The reliable  $\text{O}_2$  measurements are summarized in Fig. 3. The rate constants increase monotonically up to  $\nu=9$ , then stabilize or decrease slightly to  $\nu=12$ . The  $\nu=12$  level is the highest lying vibrational

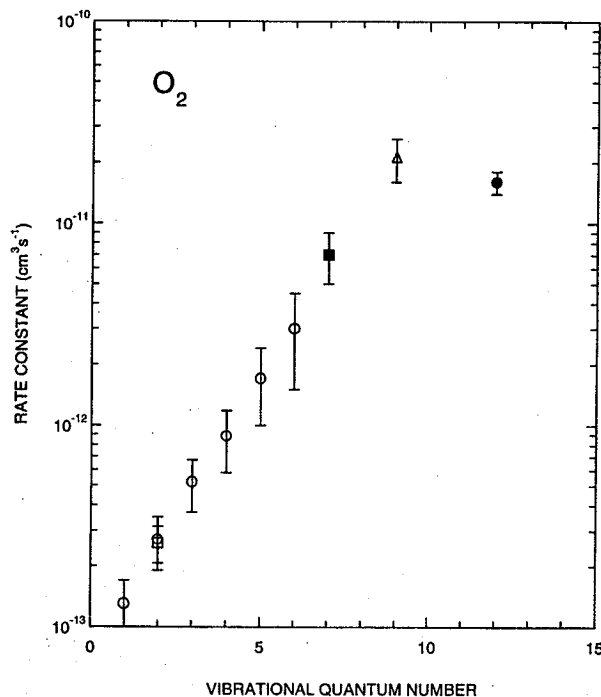


FIG. 3. Plot of the vibrational removal rate constants for  $\text{O}_2$  vs the OH vibrational level on a log scale. Open circles, Ref. 8; open square, Refs. 3 and 4; open triangle, Ref. 10; solid circle, Ref. 6; solid square, this work.

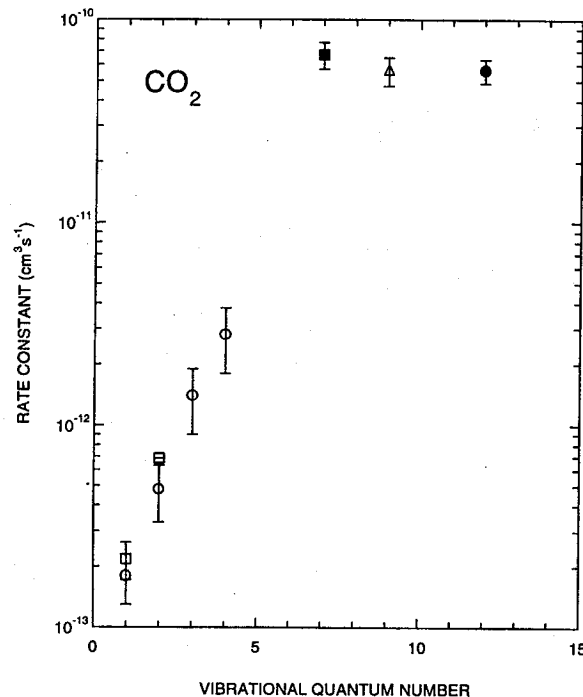


FIG. 4. Plot of the vibrational removal rate constants for  $\text{CO}_2$  vs the OH vibrational level on a log scale. Open circles, Ref. 8; open squares, Refs. 3 and 4; open triangle, Ref. 10; solid circle, Ref. 6; solid square, this work.

level that lies below the  $\nu=0$  level of the first excited doublet state of OH,  $A^2\Sigma^+$ . Single quantum relaxation out of  $\nu=12$  is about  $70 \text{ cm}^{-1}$  exothermic, while that for  $\nu=7$  is almost  $1030 \text{ cm}^{-1}$  exothermic. For  $\text{O}_2$ , no near-resonant enhancement in the magnitude of the rate constant is obvious from the vibrational level dependence. Recent trajectory calculations<sup>18</sup> find an important multiquantum relaxation pathway at high vibrational levels. The only missing data in the atmospherically important vibrational levels is that for  $\nu=8$ . Experiments on  $\nu=8, 10$ , and  $11$  are underway in this laboratory and will be presented in a future publication.<sup>19</sup> At this point we see no evidence for a maximum in the rate constant as predicted by McDade and Llewellyn if the collisional cascade model is assumed.<sup>11</sup> This again supports a multiquantum or a "sudden death" type of loss process for the higher OH vibrational levels. Measurements on  $\nu=8$  will either strengthen or weaken this conclusion. The  $\nu=7$  measurement for  $\text{O}_2$  follows the smooth vibrational level trend from the Dodd *et al.* study<sup>8</sup> and is consistent with these measurements, in which a radically different experimental approach was used. Thus, the  $\text{O}_2$  vibrational level dependence appears well understood.

For  $\text{N}_2$  the upper limit of  $6 \times 10^{-13} \text{ cm}^3 \text{s}^{-1}$  is similar to the upper limit<sup>10</sup> obtained for  $\nu=9$ ,  $5 \times 10^{-13} \text{ cm}^3 \text{s}^{-1}$ . It is smaller than the measurement<sup>6</sup> for  $\nu=12$  of  $(2.5 \pm 0.7) \times 10^{-12} \text{ cm}^3 \text{s}^{-1}$ . From these data there is no apparent resonant enhancement in the one quantum transfer process even though it is only  $255 \text{ cm}^{-1}$  exothermic for  $\nu=7$ . Data for  $\text{CO}_2$  are shown in Fig. 4. The rate constant for  $\nu=7$  is similar in magnitude to both the  $\nu=9$  and  $12$

values.<sup>6,10</sup> The vibrational removal rate increases with vibrational level for  $\nu=1-4$  and appear constant for  $\nu=7-12$ . Clearly, the unstudied vibrational levels must be examined to confirm this trend. For  $\text{CO}_2$ , the one quantum transfer into the  $\nu_3$  mode is about  $236\text{ cm}^{-1}$  exothermic for  $\nu=7$ . More work is needed on  $\text{CO}_2$  to know if this is significant. The  $\text{N}_2\text{O}$  rate constant for  $\nu=7$  is about a factor of 2 slower than for  $\text{CO}_2$ , and also about a factor of 2 slower than the only other measurement for  $\text{N}_2\text{O}$  in high vibrational levels, for  $\nu=9$ .<sup>10</sup> With only two measurements of two vibrational levels it is inappropriate to speculate on the cause of this difference. Because of their slightly different vibrational spacings, studying the similarities and differences between  $\text{CO}_2$  and  $\text{N}_2\text{O}$  will be instructive and is underway.

In conclusion, OH vibrational removal is rapidly becoming well understood using state-specific techniques. In collisions with  $\text{O}_2$ , the vibrational dependence has been examined from  $\nu=1$  to 12. Measurements on only a few vibrational levels are needed to complete this entire range. For modeling the atmosphere, the temperature dependence of OH vibrational removal below room temperature will be a critical measurement, since the temperature in the OH emitting layer varies from 150 to 230 K.

#### ACKNOWLEDGMENTS

We thank Tom Slanger and John Coxon for their helpful discussions. We gratefully acknowledge the support of this research by the National Science Foundation Aeronomy Program (ATM-9111409) and National Aeronautics and Space Administration Space Physics Program (NAGW-4017).

- <sup>1</sup>J. W. Meriwether, Jr., *J. Geophys. Res.* **94**, 14629 (1989).
- <sup>2</sup>B. J. Finlayson-Pitts and T. E. Kleindienst, *J. Chem. Phys.* **74**, 5643 (1981).
- <sup>3</sup>G. D. Greenblatt and J. R. Wiesenfeld, *J. Geophys. Res.* **87**, 11145 (1982).
- <sup>4</sup>K. J. Rensberger, J. B. Jeffries, and D. R. Crosley, *J. Chem. Phys.* **90**, 2174 (1989).
- <sup>5</sup>G. A. Raiche, J. B. Jeffries, K. J. Rensberger, and D. R. Crosley, *J. Chem. Phys.* **92**, 7258 (1990).
- <sup>6</sup>A. D. Sappey and R. A. Copeland, *J. Chem. Phys.* **93**, 5741 (1990).
- <sup>7</sup>J. A. Dodd, S. J. Lipson, and W. A. M. Blumberg, *J. Chem. Phys.* **92**, 3387 (1990).
- <sup>8</sup>J. A. Dodd, S. J. Lipson, and W. A. M. Blumberg, *J. Chem. Phys.* **95**, 5752 (1991).
- <sup>9</sup>D. V. Shalashilin, S. Y. Umanskii, and Y. M. Gershenzon, *Chem. Phys.* **168**, 315 (1992).
- <sup>10</sup>B. R. Chalamala and R. A. Copeland, *J. Chem. Phys.* **99**, 5807 (1993).
- <sup>11</sup>I. C. McDade and E. J. Llewellyn, *J. Geophys. Res.* **92**, 7643 (1987).
- <sup>12</sup>I. C. McDade, *Planet. Space Sci.* **39**, 1049 (1991).
- <sup>13</sup>R. A. Copeland, K. Knutsen, and T. G. Slanger, in *Proceedings of the International Conference on Lasers '93*, edited by V. J. Corcoran and T. A. Goldman (STS Press, McLean, VA, 1994), pp. 318.
- <sup>14</sup>T. G. Slanger and R. A. Copeland, in *Progress and Problems in Atmospheric Chemistry*, edited by J. R. Barker (World Scientific, Singapore, 1996), pp. 500-568.
- <sup>15</sup>A. D. Sappey, D. R. Crosley, and R. A. Copeland, in *Advances in Laser Science-IV*, AIP Conf. Proc. No. 191, edited by J. L. Gole *et al.* (AIP, New York, 1989), pp. 645.
- <sup>16</sup>A. D. Sappey, D. R. Crosley, and R. A. Copeland, *J. Chem. Phys.* **90**, 3484 (1990); *ibid.* **92**, 818(E) (1990).
- <sup>17</sup>J. A. Coxon, A. D. Sappey, and R. A. Copeland, *J. Molec. Spectrosc.* **145**, 41 (1991).
- <sup>18</sup>D. V. Shalashilin, A. V. Michtchenko, S. Y. Umanskii, and Y. M. Gershenzon, *J. Phys. Chem.* **99**, 11627 (1995).
- <sup>19</sup>M. J. Dyer, K. Knutsen, and R. A. Copeland (unpublished).

